



Original Research Paper

Bio-oil hydrodeoxygenation over acid activated-zeolite with different Si/Al ratio

Saharman Gea^{1,2}, Irvan Irvan^{1,3}, Karna Wijaya^{4,*}, Asma Nadia⁴, Ahmad Nasir Pulungan⁵, Junifa Layla Sihombing⁵, Rahayu Rahayu⁵

¹Cellulosic and Functional Materials Research Centre, Universitas Sumatera Utara, Jl. Bioteknologi No. 1, Medan 20155, Indonesia.

²Department of Chemistry, Faculty of Mathematics and Natural Sciences, Universitas Sumatera Utara, Jl. Bioteknologi No. 1, Medan 20155, Indonesia.

³Chemical Engineering Department, Faculty of Engineering, Universitas Sumatera Utara, Jl. Almamater Komplek USU, Medan 20155, Indonesia.

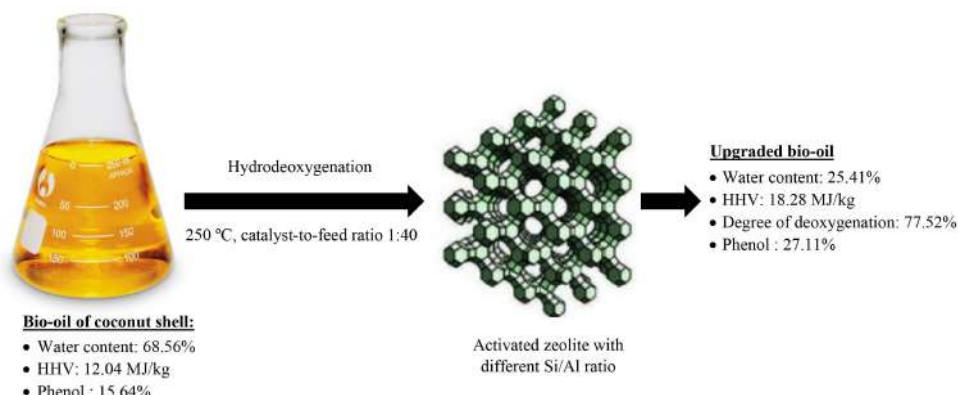
⁴Department of Chemistry, Universitas Gadjah Mada, Yogyakarta 55281, Indonesia.

⁵Department of Chemistry, Faculty of Mathematics and Natural Sciences, Universitas Negeri Medan, Jl. Willem Iskandar Pasar V Medan Estate, Medan 20221, Indonesia.

HIGHLIGHTS

- Dealumination with various acid concentrations led to different physical characteristics.
- Dealumination improved the catalytic activity of zeolite in hydrodeoxygenation (HDO).
- HDO-upgraded bio-oil had an increased HHV and decreased water content.
- Dealuminated zeolite with 5 M HCl produced the most optimal bio-oil.
- Hydrodeoxygenation of oxygenate compounds correlated with increasing phenol in bio-oil.

GRAPHICAL ABSTRACT



ARTICLE INFO

Article history:

Received 25 April 2022
Received in revised form 24 May 2022
Accepted 27 May 2022
Published 1 June 2022

Keywords:

Natural zeolite
Dealumination
Si/Al ratio
Bio-oil hydrodeoxygenation
Physicochemical properties

ABSTRACT

Bio-oil includes significant levels of oxygenate molecules, which might induce component instability and reduce its physicochemical qualities. To counteract this, the component must undergo a hydrodeoxygenation (HDO) reaction. Due to the presence of acidic active sites, zeolites have been shown to have high hydrogenation and deoxygenation capabilities. However, natural zeolite has a large number of impurities and low acidity density. Consequently, before being employed as an HDO catalyst, pretreatments such as preparation and activation are required. In this study, the catalyst used was an active natural zeolite whose acidity level varied depending on the Si/Al ratio after dealumination with 3, 5, and 7 M hydrochloric acid, proceeded by calcination with nitrogen gas flow (designated as Z3, Z5, and Z7, respectively). The results showed that dealumination and calcination of zeolite generally caused changes in its physical characteristics and components. The Z5 catalyst showed the best catalytic performance in the HDO process of bio-oil. The higher heating value (HHV) of bio-oil increased from 12 to 18 MJ/kg, the viscosity value doubled, the degree of deoxygenation increased to 77%, and the water content reduced dramatically to about one-third of that of raw bio-oil. Moreover, control compounds, such as carboxylic acids, decreased slightly, but the amount of phenol increased to about twice the content in raw bio-oil.

©2022 BRTeam CC BY 4.0

* Corresponding author at: Tel.: +62 274545188
E-mail address: karnawijaya@ugm.ac.id

Contents

| | |
|---|------|
| 1. Introduction..... | 1631 |
| 2. Materials and Methods..... | 1632 |
| 2.1. Materials..... | 1632 |
| 2.2. Zeolite preparation and activation..... | 1632 |
| 2.3. Catalyst characterization..... | 1632 |
| 2.4. Bio-oil hydrodeoxygenation..... | 1632 |
| 2.5. Bio-oil characterization..... | 1632 |
| 3. Results and Discussion..... | 1632 |
| 3.1. Functional groups in zeolite..... | 1632 |
| 3.2. Surface morphology of the catalyst..... | 1633 |
| 3.3. Elemental composition of zeolite..... | 1633 |
| 3.4. Crystallinity of the catalyst..... | 1634 |
| 3.5. Adsorption-desorption isotherm analysis..... | 1634 |
| 3.6. Catalytic performance..... | 1634 |
| 4. Conclusions and Prospects..... | 1636 |
| Acknowledgements..... | 1637 |
| References..... | 1637 |

Abbreviations

| | |
|-----|--------------------------------------|
| BET | Brunauer-Emmett-Teller |
| BJH | Barrett-Joyner-Halenda |
| DOD | Deoxygenation |
| EDX | Energy dispersion X-ray spectroscopy |
| HDO | Hydrodeoxygenation |
| HHV | Higher heating value |
| PZ | Parent zeolite |
| XRD | X-ray diffractometer |

1. Introduction

The use of bio-oil is rapidly growing, especially as wood and food preservatives. The accessible bio-oil, on the other hand, still contains significant oxygenates, which can compromise component stability. Furthermore, a high oxygen content of 35–50% can cause deteriorated physical properties, such as being corrosive and having a low heating value, high viscosity, and low chemical stability (Hiltner et al., 2010; Zhang et al., 2017; Ren and Ye, 2018).

The hydrodeoxygenation (HDO) method can be used to convert high oxygenated chemicals to phenols and derivatives, resulting in a more stable bio-oil. Guaiacol (2-methoxyphenol) is a common component of bio-oil made from lignocellulosic biomass pyrolysis. The hydrogenolysis of hydroxyl groups can transform guaiacol into methane and catechol, which can then be converted to phenols. Furthermore, *via* hydrogenolysis of methoxy groups, guaiacol can be transformed directly into phenols (Sun et al., 2013; Grilc et al., 2014; Espro et al., 2017).

Selective catalysts are required for bio-oil HDO reaction to optimize the deoxygenation of oxygenated constituents in bio-oil. Zeolites have been reported to be effective in the deoxygenation process of pyrolysis vapors, leading to decreased formation of O/C content in bio-oil (Carlson et al., 2008). Zeolites as catalysts are preferred in the HDO process because of their attractive characteristics such as large surface areas, uniform pores, hydrophobicity, modifiable acidity, and high thermal stability (Jha and Singh, 2011; De et al., 2016; Gea et al., 2020). High porosity allows compounds to diffuse into pores and access active sites quickly, improving the catalytic activity (Yoldi et al., 2019). Gea et al. (2020) reported that HDO reaction of bio-oil using active Sarulla natural zeolite with the Z3 catalyst resulted in the highest contents of phenol and its derivatives at 62.39%, with an 11.93% reduction of alkoxy compounds. The effect of pore sizes was observed by Lee et al. (2016) in HDO of guaiacol using Pt/HZSM-5 and Pt/HY catalysts. Although Pt/HZSM-5 had higher acidity than Pt/HY, it could only convert 13% of the guaiacol, while Pt/HY could convert 75%. This observation could be explained by the fact that guaiacol (kinematic diameter 0.67 nm) could more easily access the active sites of Pt/HY (porosity 0.74 nm) than Pt/HZSM-5 (porosity 80.63 nm). Garba et al. (2018) reported that the yields of bio-oil, gas, and char were slightly affected by the structure of zeolites, but the bio-oil chemical composition was highly dependent on the structure of the catalysts. Meanwhile, product distribution, coke formation, and deoxygenation rate were all influenced by the pore diameters and acidity of the catalysts. The main component of bio-oil created by catalytic pyrolysis were reportedly phenolic compounds, ketones, aromatics, and olefins (Kurnia et al., 2017).

Based on the previous research listed in Table 1, very few articles discuss the potential of natural zeolites in the HDO process, especially by examining the effect of the Si/Al ratio on the catalytic activity. In addition, most of the studies used model compounds due to the complexity of the compounds contained in crude bio-oil.

Table 1.

The latest research in hydrodeoxygenation of bio-oil compounds.

| Feed | Catalyst | Si/Al | Reactor | T (°C) | P _{H₂} | Ref. |
|---------------|-----------------|------------------------|-----------------|--------|----------------------------|--------------------------|
| Guaiacol | Pd/C-HZSM-5 | 80, 50, and 30 | Batch | 275 | 64 bar | Shafaghath et al. (2015) |
| Anisole | Al-MCM-41 | 10, 20, 40, and 60 | Fixed bed | 400 | 100 kPa | Taghvaei et al. (2021) |
| | Natural zeolite | 5 | | | | |
| | Escott zeolite | 5.7 | | | | |
| Anisole | H-BEA | 12.5 | Continuous flow | 220 | 4 MPa | Yan et al. (2021) |
| | H-MOR | 10 | | | | |
| Pyrolysis oil | FeMoP/HZSM-5 | - | Fixed bed | 450 | 65 bar | Hita et al. (2020) |
| Pyrolysis oil | Natural zeolite | 2.9, 8.6, 6.8, and 6.7 | Fixed bed | 250 | 1 atm | This work |

Therefore, natural zeolite was activated in this study using mineral acids at various concentrations to produce zeolites with different Si/Al ratios. The catalyst activity test was carried out in the bio-oil HDO process. Zeolite characteristics before and after dealumination and calcination were observed. Moreover, changes in the physicochemical properties of raw and HDO bio-oil were also observed. Carboxylic acid, phenol, and alkoxy phenol compounds were the control compounds for the HDO process. The results of this study are expected to contribute to the understanding of the pyrolytic bio-oil upgrading process using the HDO method under mild reaction conditions over active natural zeolite with different Si/Al ratios.

2. Materials and Methods

2.1. Materials

Commercial natural zeolite was purchased from CV. Bratachem Indonesia. Bio-oil was obtained from coconut shell pyrolysis. Nitrogen, oxygen, and hydrogen gases were obtained from PT Aneka Gas Medan. HCl (p.a), HNO₃ (p.a), and methanol (p.a) were purchased from Merck.

2.2. Zeolite preparation and activation

Natural zeolite was prepared by following the procedure previously reported by Sihombing et al. (2020). Zeolite was crushed and sieved at 100 mesh, and the obtained powder was soaked and washed with distilled water. Finally, the sample was dried in an oven at 120 °C. PZ was HCl activated by reflux method at 90 °C for 1 h. The HCl variations used were 3, 5, and 7 M. The precipitate was washed with deionized water until pH was neutral, followed by a heating process in an oven at 120 °C for 3 h and a calcination process at 500 °C with nitrogen gas flow. Acid activated natural zeolite was labelled as Z3, Z5, and Z7, respectively.

2.3. Catalyst characterization

The chemical composition of the catalysts was characterized by an X-Ray Fluorescence (XRF) RIGAKU-NEX QC+QuanTEZ equipped with <160eV @ Mn K-Alpha Line detector. The crystal properties were analyzed using an XRD Shimadzu 6100 Cu Kα (λ = 1.54184 Å) at 40 kV and 30 mA at 22.00 – 70.00-degree region. Surface morphology analysis was done using an SEM Zeiss EPOMH 10Zss equipped with EDX. The nitrogen adsorption-desorption test was performed with a Gas Sorption Analyzer (NOVA 1200e) Quantachrome instrument at 77 K. Specific surface area was calculated by the BET method. Pore volumes and diameters were estimated by the adsorption branch based on the BJH model. Finally, the t-plot method was used to calculate the micropore and external surface area.

2.4. Bio-oil hydrodeoxygenation

The HDO process to upgrade and stabilize bio-oil was carried out in a fixed-bed system reactor over different catalysts, including PZ, Z3, Z5, and Z7, at 250 °C, 1 atm H₂, and for 2 h. In the initial stage, the catalyst and feed (bio-oil) were weighed at a 1:40 ratio, respectively. Next, the feed and catalyst were placed in a container and into a stainless-steel reactor. After that, the reactor was placed in a furnace and heated to the specified temperature. The vapor produced from the reaction flowed through a silicon hose and passed through a condenser, where the liquid product, HDO bio-oil, was collected. During the reaction process, non-condensable gas was also produced, while coke was formed on the catalyst's surface. The yields of coke, liquid phase, and organic phase were calculated using Equations 1 and 2 (Oh et al., 2015):

$$Y_{\text{product}} (\%) = \frac{M_{\text{product}} (g)}{M_{\text{bio-oil}} (g)} \times 100 \quad \text{Eq. 1}$$

$$Y_{\text{gas}} (\%) = 100 - [Y_{\text{liquid phase}} + Y_{\text{organic phase}} + Y_{\text{coke}}] \quad \text{Eq. 2}$$

where Y_{product} and M_{product} are the yield (liquid phase, organic phase, and coke) and mass of the products, respectively.

2.5. Bio-oil characterization

Bio-oil was characterized for its compound and elementary components (C, H, O, N, S) using a CHN Analyzer LECO-CHN 628. Physicochemical properties before and after the HDO process, including water content (Metrohm 870 KF Titrino Plus), viscosity (Viscocoil 6 s brand LAUDA), acid number (titrimetric method), HHV (Sheng and Azevedo's formula), and compound composition (GC-MS-QP2010 Plus merk Shimadzu) were also analyzed.

Van Krevelen diagram was depicted using H/C and O/C atomic ratios, which were calculated from the elemental analysis of C, H, and O. The degree of DOD was estimated as follows (Eq. 3):

$$\text{DOD}(\%) = \frac{\text{MO}_{\text{raw bio-oil}} - \text{MO}_{\text{heavy oil}}}{\text{MO}_{\text{raw bio-oil}}} \times 100 \quad \text{Eq. 3}$$

where MO is the atomic O/C ratio obtained from the molar ratios of O and C levels based on the elemental analysis.

3. Results and Discussion

3.1. Functional groups in zeolite

The comparison of FTIR spectra between parent and acid-activated zeolite is presented in Figure 1. The wavenumber in the range of ~3400 cm⁻¹ indicates the stretching of the Si-O(H)-Al group. After the acid activation treatment, the transmittance (%) of IR radiation was significantly increased. This may be attributed to the depletion of water molecules bound in zeolite structures because of the calcination and oxidation reactions (Gea et al., 2020). The release of water molecules (free -OH group) is also approved due to the higher transmittance in the wavenumber range of 1600-1450 cm⁻¹ for acid-washed zeolites (Wijaya et al., 2020). Moreover, due to calcination, oxidation, and thermal effect, some functional groups were released from their bonds (Zhou et al., 2017; Ichsan et al., 2019).

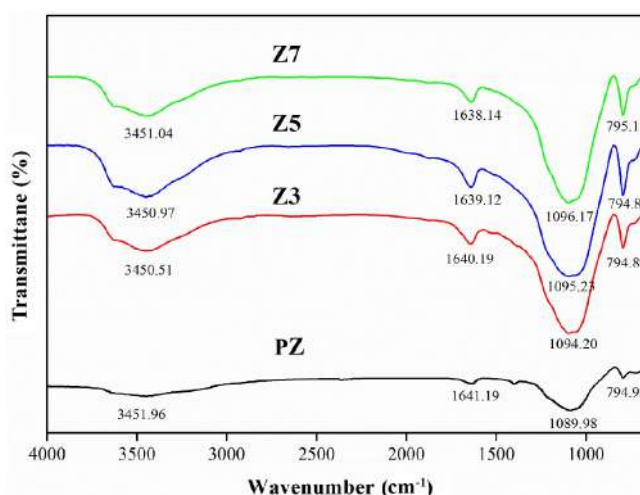


Fig. 1. Comparison of the FTIR spectra of the parent and acid-activated zeolite within the wavenumber range of 650-4000 cm⁻¹.

Zeolites containing clinoptilolite and mordenite types are reported to have strong stretching vibrations in the wavenumber range of ~1045-1070 cm⁻¹ for the Si-O-Al and Si-O-Si groups. After the dealumination stage, where some of the Al leave the zeolite framework, a shift toward higher wavenumber is observed. As the acid concentration in the activation step increases, the change in wavenumber towards higher values also increases. In addition, the higher transmission in the wavenumber range of ~790-802 cm⁻¹ shows a higher amount of Si-O/Al-O group in the acid-activated

zeolites (Triantafyllidis et al., 2001). The same results have been reported by Ates and Hardacre (2012) that acid treatment and deionization affect the wavenumber shift of functional groups.

3.2. Surface morphology of the catalyst

The surface morphology comparison between PZ and acid-activated zeolites is shown in Figure 2. There were differences in the surface morphology after the activation with mineral acid and calcination. Active zeolite tended to have single grains separated from each other, while the grains in parent zeolite were agglomerated. The Z7 catalyst had a more uniform grain size and a more homogeneous surface shape. Meanwhile, Z3 and Z5 catalysts had more diverse grain sizes. The change in the size of the zeolite particles to smaller fragments supported the BET analysis result, indicating increased external surface area.

3.3. Elemental composition of zeolite

Changes in zeolite morphology after dealumination and calcination treatment indicated the removal of some components in the zeolite. The comparison of the composition of the different zeolite samples is tabulated in Table 2.

Based on catalyst composition data presented in Table 2, there was a significant decrease in aluminium percentage after acid activation and calcination. Using the mineral acid HCl (3, 5, and 7 M), the dealumination process dissolved the Al in zeolites (Ngapa, 2017). During the activation and calcination processes, dealumination must have caused the alumina to

release from the zeolite tetrahedral framework structure outside the framework, resulting in silanol-rich species, therefore increasing the Si/Al ratio in catalysts (Ban et al., 2010; Wang et al., 2012; Fajar et al., 2020). A high Si/Al ratio would impact the stability of zeolite crystals, and as a result, the zeolite would be more resistant to heat (Ates and Hardacre, 2012).

The purpose of using HCl during the dealumination stage was to dissolve aluminium oxide from the crystal framework and force it out of the zeolite structures. Protons bound with the oxygen in the alumina ($-AlO_3-$) functional group created by acid activation treatment formed Brønsted acid sites in zeolites. The Lewis acid sites in zeolites came from the Al atom in the zeolite framework, which was formed by releasing water molecules from Brønsted sites at high temperatures. Zeolites with protonated frameworks would quickly decompose, releasing water molecules in the process. Some zeolite structures were destroyed as a result, forming Lewis acid sites. The methods of dealumination and calcination have been shown to improve acid strength and the overall number of acid sites in catalysts (Wang et al., 2018; Liu et al., 2020).

In addition, there was a decationization process during activation, where hydrochloric acid dissolved impure metals, such as Na^+ , K^+ , and Ca^{2+} , from zeolite surfaces and frameworks. In Table 2, the impurities in Z3, Z5, and Z7 catalysts were drastically reduced by almost 50% after acid and calcination treatment. The calcination process could have also contributed to removing impurities by thermal effect. This could be observed from the decrease in the percentage of impure components post-acid and calcination treatment (Guo et al., 2021).

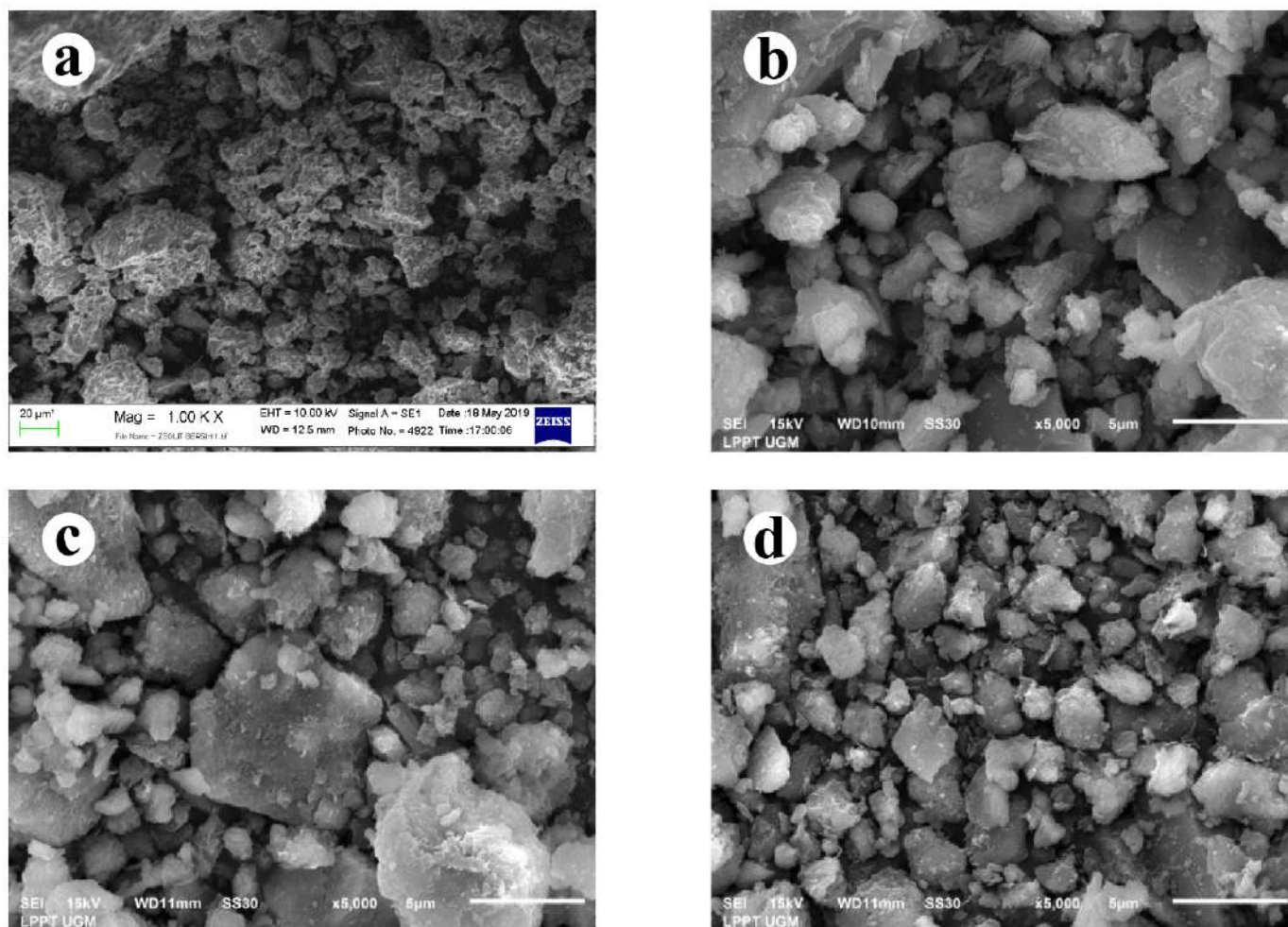


Fig. 2. Surface morphology of each catalyst; (a) PZ, (b) Z3, (c) Z5, and (d) Z7, by SEM imaging with 1000× magnification.

Table 2.
Composition of parent and activated zeolite using EDX analysis.

| Component (%) | PZ | Z3 | Z5 | Z7 |
|---------------|------|------|------|------|
| Si | 19.9 | 20.9 | 32.3 | 20.3 |
| Al | 6.86 | 2.43 | 4.75 | 3.04 |
| O | 44.4 | 61.7 | 48.2 | 57.9 |
| Impurities | 28.8 | 14.9 | 14.8 | 18.8 |
| Si/Al | 2.90 | 8.60 | 6.79 | 6.67 |

3.4. Crystallinity of the catalyst

The diffractograms of parent and acid-activated zeolites are summarized in **Figure 3**. These peaks characterize natural zeolite types of mordenite and clinoptilolite, including peaks indicating mordenite in the $2\theta = 20.68^\circ$, 22.07° , 27.71° , and 30.68° regions, while the characteristic peaks of clinoptilolite can be seen in the $2\theta = 9.70^\circ$, 13.30° , 25.70° , 26.24° , 29.93° , and 35.62° regions. The diffraction patterns of the catalysts did not significantly contrast with one another. However, some increase and decrease in intensity at some of the peaks, especially in the zeolite-characteristic area between $2\theta = 20^\circ$ – 30° , can be observed. The high characteristic peak intensity in zeolites was directly related to the crystalline properties. The presence of zeolite peaks and the degree of crystallinity are summarized in **Table 3**.

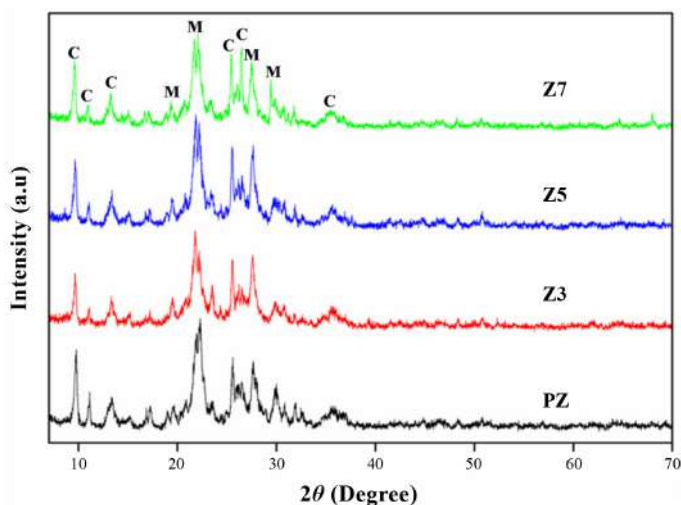


Fig. 3. The diffractograms of parent and acid-activated zeolites; C denotes Clinoptilolite, and M stands for Mordenite.

Table 3.
Comparison of peak intensities for parent and acid-activated zeolites

| 2θ ($^\circ$) | Intensity | | | |
|-----------------------------|-----------|------|------|------|
| | PZ | Z3 | Z5 | Z7 |
| 22.0707 | 209 | 164 | 174 | 179 |
| 23.4400 | 33 | 47 | 87 | 45 |
| 25.7000 | 88 | 75 | 87 | 91 |
| 26.2400 | 76 | 50 | 47 | 79 |
| 27.7133 | 110 | 114 | 123 | 124 |
| Degree of crystallinity (%) | 42.9 | 46.8 | 47.8 | 49.5 |

Acid treatment increased the degree of crystallinity in zeolites. This was possible because the dealumination process dissolved most of the impurities in zeolite surfaces and pores. Therefore, with cleaner surfaces and pores, X-ray

diffraction was more intense. A similar finding was reported by [Wijaya et al. \(2013\)](#), who employed acid activation using sulfuric acid 1 M and observed increased zeolite crystallinity, indicating that impurities in the zeolite were removed and a more regular tetrahedral framework was formed. The water trapped in zeolite structures was evaporated during the calcination process, allowing them to become more crystalline ([Zhou et al., 2017](#)). The calcination process also oxidized contaminants and opened up the zeolite pores. Furthermore, removing non-framework Al species increased the Si/Al ratio and zeolite crystallinity ([Feng et al., 2019](#); [Wang et al., 2019](#)).

3.5. Adsorption-desorption isotherm analysis

Adsorption-desorption isotherm graphs of the parent and acid-activated zeolites are shown in **Figure 4**. Based on the IUPAC classification, the isotherm graph was classified as type IV with a hysteresis loop at P/P_0 between 0.4–1.0. The presence of a hysteresis loop indicated meso and micro-sized pores in the zeolites.

The surface area, pore diameter, and total volume of the parent and activated zeolites are tabulated in **Table 4**. After dealumination and calcination processes, surface area, pore diameter, and total pore volume increased. Dealumination causes an increase in the Si/Al ratio, an increase in the specific surface area, and a decrease in the concentration of Brønsted and Lewis acid sites ([Horáček et al., 2013](#)). In this study, the Z5 catalyst showed the highest percentage of micro surface area reduction accompanied by the most significant increase in pore size. In contrast, catalysts Z3 and Z7 showed a larger surface area but slightly smaller pore diameter. The increase in specific and external surface areas accompanied by a decrease in the micro surface area indicated that the Z3, Z5, and Z7 catalysts were damaged in the initial PZ frame due to dealumination. This also causes a widening of the pore size of the active acid catalyst by up to twice that of the parent zeolite.

The external surface area of zeolite was increased after acid treatment ([Fajar et al., 2020](#)). As a result of the Al framework breakdown, the micro surface area decreased simultaneously with the increase in the external surface. As a result, zeolites formed mesoporous structures ([Ates and Hardacre, 2012](#)). With the elimination of amorphous Al species that previously occupied the zeolite micropores, thermal impacts during calcination also contributed to the development of secondary mesopores ([Park et al., 2005](#); [Lazaridis et al., 2018](#)). The presence of mesoporous catalysts would improve bulk molecule access to the catalyst pores while also increasing product conversion.

Table 4.
Surface area, pore diameter, and total volume of parent and activated zeolites

| Sample | SBET (m^2/g) | S_{micro} (m^2/g) ^a | S_{external} (m^2/g) ^a | V_{total} (cc/g) | Average pore diameter (nm) |
|--------|--------------------------------|---|--|--------------------------------------|----------------------------|
| PZ | 18.5 | 3.14 | 15.3 | 0.078 | 1.60 |
| Z3 | 21.1 | 2.37 | 18.7 | 0.087 | 3.12 |
| Z5 | 20.5 | 0.23 | 20.3 | 0.082 | 3.56 |
| Z7 | 23.4 | 2.06 | 21.3 | 0.081 | 3.12 |

^a t-plot method

3.6. Catalytic performance

The catalyst activity test was carried out for the bio-oil HDO process, where the proportions of the liquid phase, organic phase, coke, and gas produced were calculated. The yield distribution of the products is presented in **Figure 5**.

According to the yield distribution diagram depicted in **Figure 5**, the liquid phase was the most abundant product generated, followed by the organic phase and gas. A relatively small amount of coke formed, which accounted for no more than 1% of the total product conversion. Bio-oil catalyzed by Z7 tended to produce a higher liquid phase percentage of almost 80%, thus leading to a lower organic phase yield ([Lazaridis et al., 2018](#)). High liquid phase yield indicated the occurrence of dehydration and

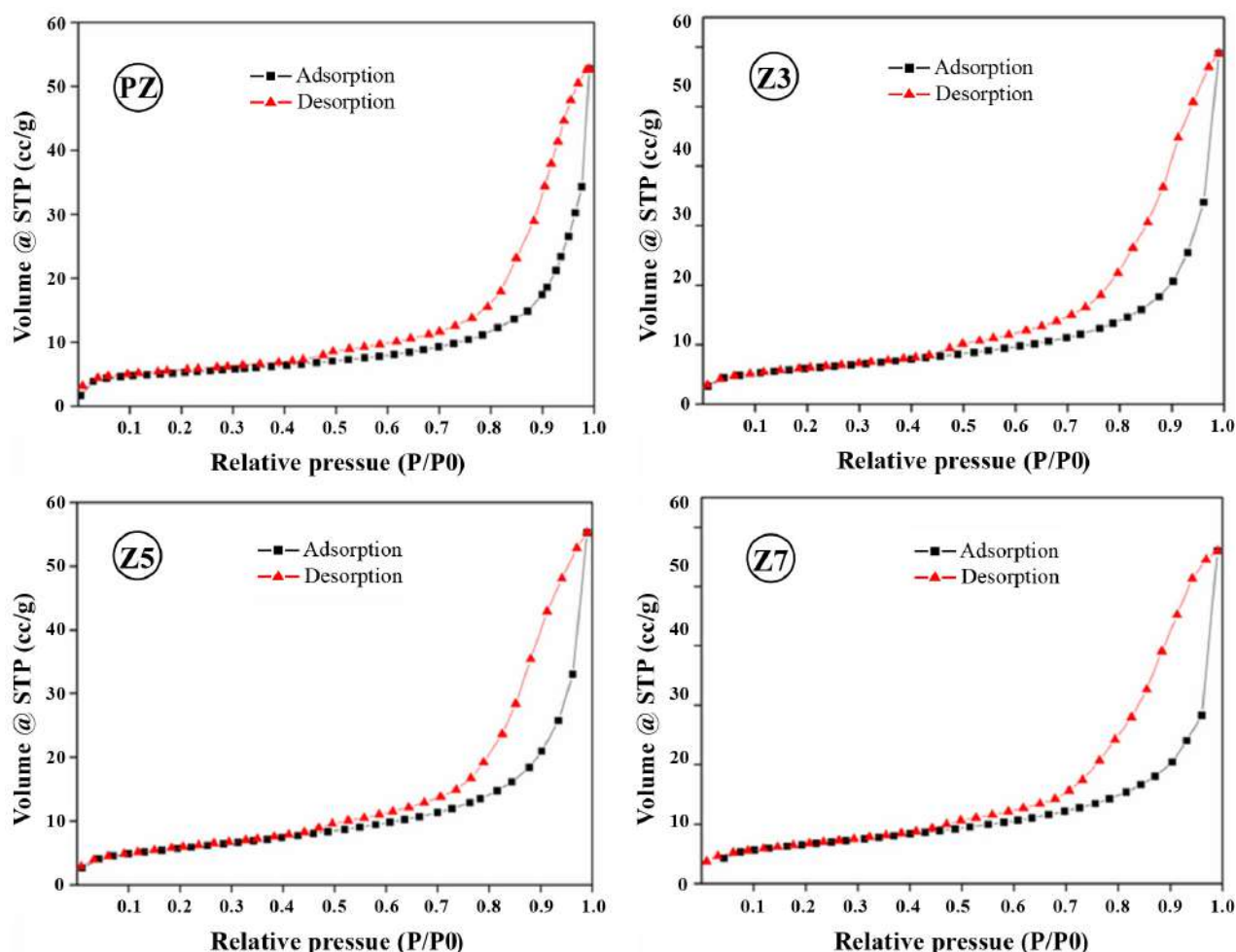


Fig. 4. Adsorption-desorption isotherm graphs of the parent and acid-activated zeolites.

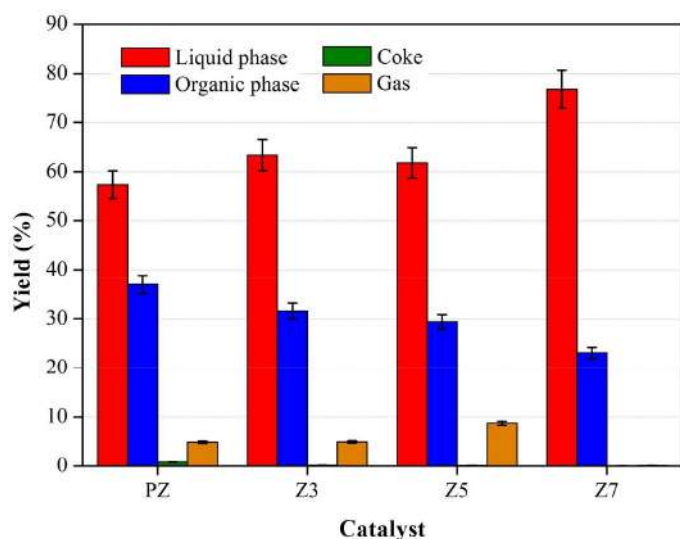


Fig. 5. The product distribution of HDO bio-oil using the parent and activated zeolites as the catalyst.

carboxylation as the dominant reaction pathways (Palizdar and Sadrameli, 2019). Except for the Z7 catalyst, where the gas generated was less than 1%, the proportion of organic phase produced decreased as the concentration of mineral acid applied in the catalyst activation process increased.

The comparison of physicochemical properties of raw bio-oil and the HDO bio-oil over various catalysts is summarized in Table 5. There were significant differences between the raw and HDO bio-oils in several test parameters such as HHV, viscosity, and water content.

In general, the properties of bio-oil catalyzed by zeolites improved. However, Z5 and Z7 catalysts showed more remarkable physicochemical properties than the other two catalysts. This could be seen in the increased HHV from 12 to 18 MJ/kg. Meanwhile, viscosity values increased by over twice the raw bio-oil, water content decreased drastically by almost one-third of the water content in the raw bio-oil, and the degree of deoxygenation could reach up to 77%. The pH value was proportional to the acid number of bio-oil. Water content was correlated to viscosity and HHV, where the lower the water content, the higher the viscosity and HHV.

Based on the data tabulated in Table 5, the molar ratios of H/C and O/C were reduced after the HDO process, both with PZ catalyst and acid-active catalyst. An increasing H/C value indicates a tendency for the HDO reaction to occur through the hydrogenation reaction pathway, but in this case, the H/C value decreases after HDO. This phenomenon is an indication that the hydrogenation process is not the dominant pathway. Meanwhile, the reduced O/C molar ratio indicates a deoxygenation reaction (Bi et al.,

2014; Serhan et al., 2019). The bio-oil catalyzed by the four catalysts showed a significant decrease in the molar ratio of O/C, especially in the case of the Z5 catalyst, which showed the most drastic reduction of over 70%. This correlates with the DOD data in Table 5.

Table 5.
Properties of raw bio-oil and HDO bio-oil.

| Properties | Raw bio-oil | PZ | Z3 | Z5 | Z7 |
|---------------------------------|-------------|------|------|------|------|
| <i>Elemental analysis (wt%)</i> | | | | | |
| C | 13.1 | 21.8 | 25.8 | 39.3 | 38.1 |
| H | 9.76 | 9.14 | 9.07 | 8.05 | 8.41 |
| N | 0.03 | 0.09 | 0.23 | 0.53 | 0.53 |
| O ^a | 77.1 | 69.0 | 64.9 | 52.1 | 53.0 |
| HHV (MJ/kg) ^b | 12.0 | 14.1 | 15.2 | 18.3 | 18.2 |
| Viscosity (mm ² s) | 1.16 | 1.50 | 1.85 | 3.35 | 3.31 |
| Water content (%) | 68.6 | 67.7 | 64.8 | 25.4 | 26.6 |
| Acid number (mg NaOH/g oil) | 156 | 130 | 144 | 142 | 145 |
| pH | 1.8 | 1.9 | 1.8 | 1.8 | 1.8 |
| DOD | - | 46.2 | 57.3 | 77.5 | 76.4 |
| H/C | 8.95 | 5.03 | 4.23 | 2.46 | 2.65 |
| O/C | 4.42 | 2.37 | 1.88 | 0.99 | 1.04 |

^a Calculated by the difference in percentage.

^b High heating value was calculated by using the following formula:
HHV (MJ/kg) = 1.3675 + (0.3137 C) + (0.7009 H) + (0.0318 O)

The physical properties and components of zeolites were frequently altered by dealumination and calcination. During the dealumination process, different mineral acid molar concentrations were applied, resulting in zeolites with varied Si/Al ratios, which would influence the acid density of the catalyst. The presence of Brønsted and Lewis acid sites in the activated zeolites affected the reaction pathways that each active site facilitated. Furthermore, zeolite properties such as surface morphology, surface area, and pore size influenced the access to active sites where conversion reactions took place.

In general, the Z7 catalyst exhibited superior properties in terms of crystallinity, Si/Al ratio, and surface area. Dealumination with a 7 M mineral acid concentration dissolved more aluminium from the zeolite framework, resulting in a considerable rise in the Si/Al ratio. This, in turn, resulted in a cleaner surface morphology of the Z7 catalyst, with homogenous small grains, resulting in a higher specific surface area. As the concentration of mineral acid in the dealumination process rose, the degree of crystallinity grew in a linear relationship with the Si/Al ratio.

The Z5 catalyst performed better in the HDO bio-oil process than the Z7 catalyst, despite having lower crystallinity, surface area, and Si/Al ratio. This could be ascribed to the high Si/Al ratio in Z7, encouraging the catalyst to be more hydrophobic. This, however, would have been advantageous if the resulting HDO product was a nonpolar compound such as alkane hydrocarbons and their derivatives. But in this case, the stabilization process was aimed at oxygenated compounds and carboxylic acids, which are semi-polar and polar. In addition, the lower Si/Al molar ratio raises the acidity of the zeolite, which helps the catalyst to enhance the rate of bio-oil deoxygenation. This finding was supported by the degree of deoxygenation, where the bio-oil catalyzed by Z5 had higher DOD than the bio-oil catalyzed by Z7. Similar results were reported by Zhang et al. (2014), where the catalyst HZSM-5 with a Si/Al ratio of 12.5 showed better catalytic performance in converting 2-methoxy-4-propylphenol into hydrocarbons than HZSM-5 with a larger Si/Al molar ratio. As a result, raising the acid concentration to 7 M altered the physical properties of zeolite, but it did not influence component stability or acid and oxygenated compound conversion in HDO bio-oil.

Another assumption that can explain the good catalytic activity of the Z5 catalyst was its larger pore size than the other catalysts. The large pore size facilitates the diffusion process and overcomes the adsorption limitations for larger molecules (Wang et al., 2013).

Figure 6 presents the chemicals found in the organic phase of bio-oil. The main bio-oil components were carboxylic acids, alkoxy phenol, and phenols.

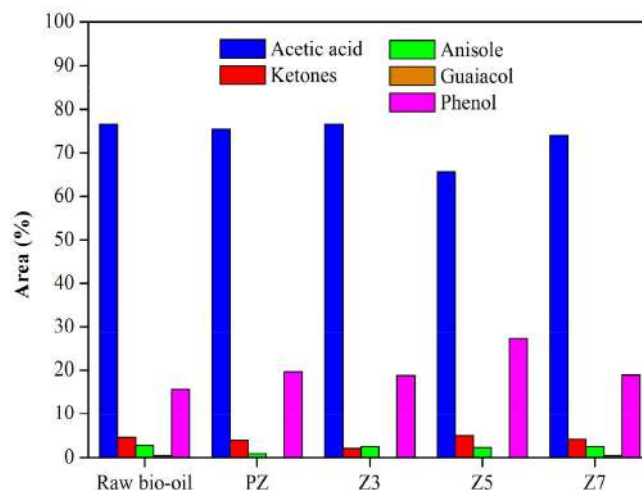


Fig. 6. Main components of the raw bio-oil and HDO products.

After the HDO process, acetic acid, which was the primary ingredient of raw bio-oil at 76%, was gradually decreased, with the highest drop in the bio-oil catalyzed by the Z5 catalyst. Meanwhile, phenol content increased by almost double in the bio-oil catalyzed by Z5. This result was correlated with the high degree of deoxygenation in Z5-catalyzed bio-oil, where oxygenated molecules were converted to phenol. The high carboxylic acid content of the bio-oil catalyzed by Z5 gradually reduces after HDO. Compared with the other catalysts, the degree of deoxygenation of bio-oil catalyzed by Z5 was also the greatest. Therefore, it can be indicated that deoxygenation was the dominant reaction. Carboxylic acid deoxygenation usually occurs via decarboxylation and ketonization reactions. In the decarboxylation pathway, carboxylic acids produce CO₂ and CH₄ (Palizdar and Sadrameli, 2019). This is supported by the distribution of the resultant HDO products (Fig. 6), which shows that the Z5 catalyst produces the largest gas product (almost 10%). This result also supports a linear relationship when it is associated with the H/C molar ratio (Table 5), where the smallest ratio is indicated by the bio-oil catalyzed by Z5, which is thought to have a lot of hydrogen coming out as methane gas. In addition, alkoxy phenol produced from pyrolysis of lignin undergoes demethylation and cleavage of methoxyl bonds over the Brønsted acid site.

In this study, guaiacol and anisole underwent demethoxylation and demethylation, respectively and produced phenol (Fig. 7). GC-MS analysis data showed the absence of the compound in bio-oil after HDO, except in bio-oil catalyzed by Z7. Product distribution data also showed the presence of a gas phase formed and increased phenol content during the HDO process over acid-activated catalysts.

4. Conclusions and Prospects

Dealumination and calcination of zeolite generally changed its physical characteristics and components. The increase in acid concentration up to 7 M modified the physical characteristics of zeolite but did not enhance component stability or the conversion of acid and oxygenated components in the HDO of bio-oil. Z5 catalyst showed the best catalytic performance in the HDO process of bio-oil. The HHV of bio-oil increased from 12 to 18 MJ/kg; the viscosity value doubled, and the degree of deoxygenation was high at 77%, while the water content decreased drastically to almost one-third of the water content in the raw bio-oil. The control compounds, including carboxylic acids, were slightly reduced, but the percentage of phenol increased to almost double its content in the raw bio-oil after the catalysis by Z5. This was correlated with the high degree of deoxygenation in Z5-catalyzed bio-oil, indicating that the oxygenated compound was converted to phenol.

This study highlights that a catalyst with a certain Si/Al ratio and acidity can affect the catalytic activity in the HDO of bio-oil under mild conditions.

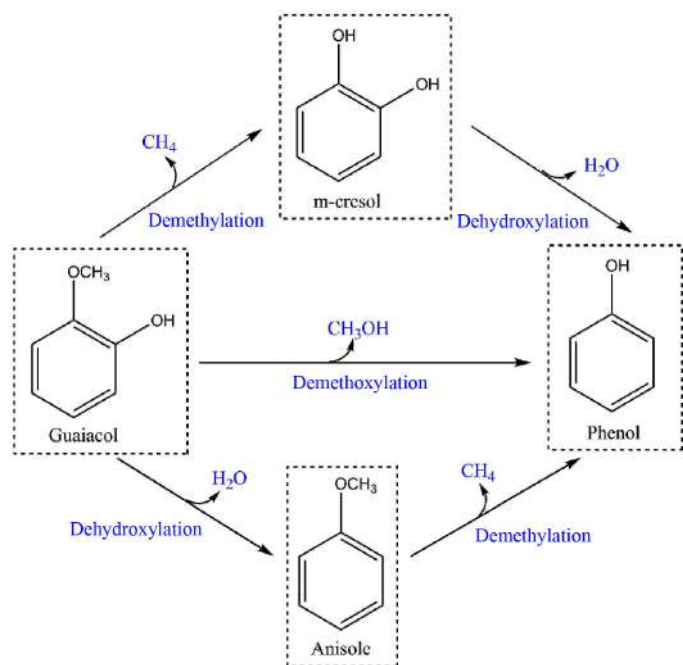


Fig. 7. Proposed reaction pathways for the hydrodeoxygenation (HDO) of guaiacol and anisole.

Further research is needed to see the effect of variations in the Si/Al ratio of natural zeolite, which are smaller or larger than that used in this study, on their catalytic performance. In addition, technology development needs to be carried out to reduce bio-oil viscosity, such as using solvents or optimizing process conditions during the reaction.

Acknowledgements

The authors would like to thank the Ministry of Education and Culture of the Republic of Indonesia for funding this research under the World Class University Program scheme of Universitas Sumatera Utara Year 2020, with the grant number 1879/UN5.1.R/SK/PPM/2020.

References

- [1] Ates, A., Hardacre, C., 2012. The effect of various treatment conditions on natural zeolites: ion exchange, acidic, thermal and steam treatments. *J. Colloid Interface Sci.* 372(1), 130-140.
- [2] Ban, S., Van Laak, A.N.C., Landers, J., Neimark, A.V., De Jongh, P.E., De Jong K.P., Vlught, T.J.H., 2010. Insight into the effect of dealumination on mordenite using experimentally validated simulations. *J. Phys. Chem. C* 114(5), 2056-2065.
- [3] Bi, Y., Wang, G., Shi, Q., Xu, C., Gao, J., 2014. Compositional changes during hydrodeoxygenation of biomass pyrolysis oil. *Energy Fuels* 28(4), 2571-2580.
- [4] Carlson, T.R., Vispute, T.P., Huber, G.W., 2008. Green gasoline by catalytic fast pyrolysis of solid biomass derived compounds. *ChemSusChem Chem. Sustainability Energy Mater.* 1(15), 397-400.
- [5] De, S., Dutta, S., Saha, B., 2016. Critical design of heterogeneous catalysts for biomass valorization: current thrust and emerging prospects. *Catal. Sci. Technol.* 6(20), 7364-7385.
- [6] Espro, C., Gumina, B., Paone, E., Mauriello, F., 2017. Upgrading lignocellulosic biomasses: hydrogenolysis of platform derived molecules promoted by heterogeneous Pd-Fe catalysts. *Catalysts* 7(3), 78.
- [7] Fajar, A.T.N., Nurdin, F.A., Mukti, R.R., Subagjo, Rasrendra, C.B., Kadja, G.T.M., 2020. Synergistic effect of dealumination and ceria impregnation to the catalytic properties of MOR zeolite. *Mater. Today Chem.* 17, 100313.
- [8] Feng, A., Yu, Y., Mi, L., Cao, Y., Yu, Y., Song, L., 2019. Synthesis and characterization of hierarchical Y zeolites using NH_4HF_2 as dealumination agent. *Microporous Mesoporous Mater.* 280, 211-218.
- [9] Garba, M.U., Musa, U., Olugbenga, A.G., Mohammad, Y.S., Yahaya, M., Ibrahim, A.A., 2018. Catalytic upgrading of bio-oil from bagasse: thermogravimetric analysis and fixed bed pyrolysis. *Beni-Suef Univ. J. Basic Appl. Sci.* 7(4), 776-781.
- [10] Gea, S., Haryono, A., Andriyani, A., Sihombing, J.L., Pulungan, A.N., Nasution, T., Rahayu, R., Hutapea, T.A., 2020. The stabilization of liquid smoke through hydrodeoxygenation over nickel catalyst loaded on sarulla natural zeolite. *Appl. Sci.* 10(12), 4126.
- [11] Grilc, M., Likozar, B., Levec, J., 2014. Hydrodeoxygenation and hydrocracking of solvolyzed lignocellulosic biomass by oxide, reduced and sulphide form of NiMo, Ni, Mo and Pd catalysts. *Appl. Catal., B* 150-151, 275-87.
- [12] Guo, X., Guo, L., Zeng, Y., Kosol, R., Gao, X., Yoneyama, Y., Yang, G., Tsubaki, N., 2021. Catalytic oligomerization of isobutyl alcohol to jet fuels over dealuminated zeolite Beta. *Catal. Today* 368, 196-203.
- [13] Hiltten, R.N., Das, K.C., 2010. Comparison of three accelerated aging procedures to assess bio-oil stability. *Fuel* 89(10), 2741-2749.
- [14] Hita, I., Cordero-Lanzac, T., Bonura, G., Frusteri, F., Bilbao, J., Castaño, P., 2020. Dynamics of carbon formation during the catalytic hydrodeoxygenation of raw bio-oil. *Sustain. Energy Fuels* 4(11), 5503-5512.
- [15] Horáček, J., Št'Ávová, G., Kelbichová, V., Kubička, D., 2013. Zeolite-Beta-supported platinum catalysts for hydrogenation/hydrodeoxygenation of pyrolysis oil model compounds. *Catal. Today* 204, 38-45.
- [16] Ichsan, G.M.H.A., Nugrahaningtyas, K.D., Widjonarko, D.M., Rahmawati, F., 2019. Structure and morphology of the (Ni, Co) Mo/Indonesian natural zeolite. *IOP Conf. Ser. Mater. Sci. Eng.* 578(1), 012009.
- [17] Jha, B., Singh, D.N., 2011. A review on synthesis, characterization and industrial applications of flyash zeolites. *J. Mater. Educ.* 33(1-2), 65-132.
- [18] Kurnia, I., Karnjanakom, S., Bayu, A., Yoshida, A., Rizkiana, J., Prakoso, T., Abudula, Kurnia, I., Karnjanakom, S., Bayu, A., Yoshida, A., Rizkiana, J., Prakoso, T., Abudula, A., Guan, G., 2017. *In-situ* catalytic upgrading of bio-oil derived from fast pyrolysis of lignin over high aluminum zeolites. *Fuel Process. Technol.* 167, 730-737.
- [19] Lazaridis, P.A., Fotopoulos, A.P., Karakoulia, S.A., Triantafyllidis, K.S., 2018. Catalytic fast pyrolysis of kraft lignin with conventional, mesoporous and nanosized ZSM-5 zeolite for the production of alkylphenols and aromatics. *Front. Chem.* 6, 295.
- [20] Lee, H., Kim, H., Yu, M.J., Ko, C.H., Jeon, J.K., Jae, J., Park, S.H., Jung, S., Park, Y., 2016. Catalytic Hydrodeoxygenation of Bio-oil Model Compounds over Pt/HY Catalyst. *Sci. Rep.* 6(1), 1-8.
- [21] Liu, P., Li, Z., Liu, X., Song, W., Peng, B., Zhang, X., Nie, S., Zeng, P., Zhang, Z., Gao, Z., Shen, B., 2020. Steaming driven chemical interactions of ZnCl_2 with Y zeolite framework, its regulation to dealumination/silicon-healing as well as enhanced availability of Brønsted acidity. *ACS Catal.* 10(16), 9197-9214.
- [22] Ngapa, Y.D., 2017. Study of the acid-base effect on zeolite activation and its characterization as adsorbent of methylene blue dye. *JKPK (Jurnal Kimia dan Pendidikan Kimia)* 2(2), 90-96.
- [23] Oh, S., Hwang, H., Choi, H.S., Choi, J.W., 2015. The effects of noble metal catalysts on the bio-oil quality during the hydrodeoxygenative upgrading process. *Fuel* 153, 535-543.
- [24] Palizdar, A., Sadrameli, S.M., 2019. Catalytic upgrading of biomass pyrolysis oil over tailored hierarchical MFI zeolite: effect of porosity enhancement and porosity-acidity interaction on deoxygenation reactions. *Renew. Energy* 148, 674-688.
- [25] Park, J., Wang, J., Hong, S., Wee, C., 2005. Effect of dealumination of zeolite catalysts on methylation of 2-methylnaphthalene in a high-pressure fixed-bed flow reactor. *Appl. Catal., A* 292, 68-75.

- [26] Ren S., Ye, X.P., 2018. Stability of crude bio-oil and its water-extracted fractions. *J. Anal. Appl. Pyrolysis*. 132, 151-162.
- [27] Serhan, M., Sprowls, M., Jackmeyer, D., Long, M., Perez, I.D., Maret, W., Tao, N., Forzani, E., 2019. Total iron measurement in human serum with a smartphone. 2019 AIChE Annu. Meet. Am. Inst. Chem. Eng.
- [28] Shafaghath, H., Rezaei P.S., Daud, W.M.A.W., 2015. Catalytic hydrogenation of phenol, cresol and guaiacol over physically mixed catalysts of Pd/C and zeolite solid acids. *RSC Adv.* 5(43), 33990-33998.
- [29] Sihombing, J.L., Gea, S., Wirjosentono, B., Agusnar, H., Pulungan, A.N., Herlinawati, H., Yusuf, M., Hutapea, Y.A., 2020. Characteristic and catalytic performance of Co and Co-Mo metal impregnated in sarulla natural zeolite catalyst for hydrocracking of MEFA rubber seed oil into biogasoline fraction. *Catalysts*. 10(1), 121.
- [30] Sun, J., Karim, A.M., Zhang, H., Kovarik, L., Li, X.S., Hensley, A.J., McEwen, J., Wang, Y., 2013. Carbon-supported bimetallic Pd-Fe catalysts for vapor-phase hydrodeoxygenation of guaiacol. *J. Catal.* 306, 47-57.
- [31] Taghvaei, H., Moaddeli, A., Khalafi-Nezhad, A., Iulianelli, A., 2021. Catalytic hydrodeoxygenation of lignin pyrolytic-oil over Ni catalysts supported on spherical Al-MCM-41 nanoparticles: effect of Si/Al ratio and Ni loading. *Fuel*. 293, 120493.
- [32] Triantafyllidis, C.S., Vlessidis, A.G., Nalbandian, L., Evmiridis, N.P., 2001. Effect of the degree and type of the dealumination method on the structural, compositional and acidic characteristics of H-ZSM-5 zeolites. *Microporous Mesoporous Mater.* 47(2-3), 369-388.
- [33] Wang, W., Zhang, W., Chen, Y., Wen, X., Li, H., Yuan, D., Guo, Q., Ren, S., Pang, X., Shen, B., 2018. Mild-acid-assisted thermal or hydrothermal dealumination of zeolite beta, its regulation to Al distribution and catalytic cracking performance to hydrocarbons. *J. Catal.* 362, 94-105.
- [34] Wang, X., Ozdemir, O., Hampton, M.A., Nguyen, A.V., Do, D.D., 2012. The effect of zeolite treatment by acids on sodium adsorption ratio of coal seam gas water. *Water Res.* 46(16), 5247-5254.
- [35] Wang, X., Zhu, S., Wang, S., He, Y., Liu, Y., Wang, J., Fan, W. and Lv, Y., 2019. Low temperature hydrodeoxygenation of guaiacol into cyclohexane over Ni/SiO₂ catalyst combined with H β zeolite. *RSC Adv.* 9(7), 3868-3876.
- [36] Wang, Y., Wu, J., Wang, S., 2013. Hydrodeoxygenation of bio-oil over Pt-based supported catalysts: Importance of mesopores and acidity of the support to compounds with different oxygen contents. *RSC Adv.* 3(31), 12635-12640.
- [37] Wijaya, K., Baobalabuana, G., Trisunaryanti, W., Syoufian, A., 2013. Hydrocracking of palm oil into biogasoline Catalyzed by Cr/natural zeolite. *Asian J. Chem.* 25(16), 8981-8986.
- [38] Wijaya, K.A.R.N.A., Utami, M.A.I.S.A.R.I., Syoufian, A.K.H.M.A.D., Hidayatullah, L.U.T.H.F.A.N., 2020. Preparation of calcium oxide/zeolite nanocomposite and its application to improve the quality of patchouli oil. *Key Eng. Mater.* 849, 119-124.
- [39] Yan, P., Kennedy, E., Stockenhuber, M., 2021. Natural zeolite supported Ni catalysts for hydrodeoxygenation of anisole. *Green Chem.* 23(13), 4673-4684.
- [40] Yoldi, M., Fuentes-Ordoñez, E.G., Korili, S.A., Gil, A., 2019. Zeolite synthesis from industrial wastes. *Microporous Mesoporous Mater.* 287, 183-191.
- [41] Zhang, C., Xing, J., Song, L., Xin, H., Lin, S., Xing, L., Li, X., 2014. Aqueous-phase hydrodeoxygenation of lignin monomer eugenol: influence of Si/Al ratio of HZSM-5 on catalytic performances. *Catal. Today*. 234, 145-152.
- [42] Zhang, L., Yin, R., Mei, Y., Liu, R., Yu, W., 2017. Characterization of crude and ethanol-stabilized bio-oils before and after accelerated aging treatment by comprehensive two-dimensional gas-chromatography with time-of-flight mass spectrometry. *J. Energy Inst.* 90(4), 646-659.
- [43] Zhou, W., Liu, M., Zhang, Q., Wei, Q., Ding, S., Zhou, Y., 2017. Synthesis of NiMo catalysts supported on gallium-containing mesoporous Y zeolites with different gallium contents and their high activities in the hydrodesulfurization of 4, 6-dimethyldibenzothiophene. *ACS Catal.* 7(11), 7665-7679.



Saharman Gea, PhD, is currently the head of Cellulosic and Functional Materials Research Centre, Universitas Sumatera Utara, and a senior lecturer at the same university. He received his PhD degree in nanotechnology material from the Queen Mary University of London in 2011. His bachelor's and master's degrees were completed at Universitas Sumatera Utara in 1997 and 2000, respectively. His research interests relate to nanomaterial and biomaterial, particularly in synthesis, nanostructure and properties, and application of nanomaterials, such

as cellulose, nanocatalyst, and carbon nanomaterial. He has authored and co-authored several articles in reputable journals such as *Polymers*, *Biomolecules*, *BioResources*, and *Journal of Energy and Environmental Engineering*. He also holds some approved patents.



Prof. Irvan is a senior lecturer in the Department of Chemical Engineering, Universitas Sumatera Utara. He received a doctorate in Environment and Life Engineering from Toyohashi University of Technology, Japan. He has been serving as a Professor since 2018 and currently serves as the Head of the Ecology Laboratory in the same department. His current research interests are anaerobic digestion, composting, biogas upgrading, and membrane technology. Some works of Prof. Irvan have been published in various

journals, while some have been patented. His Google Scholar profile can be found at the following link:

https://scholar.google.com/citations?hl=id&user=CqMOSUoAAAAJ&view_op=list_works&sortBy=pupdate.



Prof. Karna Wijaya obtained a BSc degree from the Department of Chemistry of the Faculty of Mathematics and Natural Sciences, Universitas Gadjah Mada in 1987, a Master of Engineering degree in Applied Chemistry from the School of Science and Engineering, Waseda University, Tokyo, Japan in 1993 and a Doctorate in Chemistry from the Technical University of Braunschweig, Germany in 1999. He has been serving as a professor since 2008, and he currently serves as the Head of Physical Chemistry, Department of Chemistry, Faculty of Mathematics and Natural Sciences, Gadjah Mada University and the Head of Physical Chemistry Division, Indonesian Chemical Society. He has published several scientific articles in international journals such as *Fuel*, *Mater. Renew. Sustain. Energy*, *Arabian Journal of Chemistry*, *Sustainable Environment Research*, *Applied Clay Science*, *International Journal of Applied Chemistry*, etc. Some of the works by Prof. Karna Wijaya have also been patented. He is also actively involved as an author of several books published by Gadjah Mada University Press and the Center for Energy Studies, Universitas Gadjah Mada.



Dr. Ahmad Nasir Pulungan, M.Sc., obtained his bachelor's degree from the Department of Chemistry of the Faculty of Mathematics and Natural Sciences, Universitas Sumatera Utara in 2004, and his Master of Science in Physical Chemistry from the Department of Chemistry of the Faculty of Mathematics and Natural Sciences, Universitas Gadjah Mada in 2011. In 2020, he was awarded his Doctorate in Chemistry from Universitas Sumatera Utara. He has been a chemistry lecturer at Universitas Negeri Medan Medan since

2012. His research covers the fields of catalysts, renewable energy, and membrane fuel cells.



Asma Nadia, M.Sc., got her bachelor's degree from the Department of Chemistry, Universitas Lambung Mangkurat and completed her master's degree in the catalysis field from the Department of Chemistry, Universitas Gadjah Mada. Her research interests focus on developing nanostructured materials and composites for heterogeneous catalysis to tackle the problems of global warming and renewable energy resources. She has published several scientific articles in international journals. Her Google Scholar profile can be found at the

following link:

https://scholar.google.com/citations?hl=en&user=mbF9vN8AAAAJ&view_op=list_works&sortby=pubdate.



Dr. Junifa Layla Sihombing, M.Sc obtained her bachelor's degree from the Department of Chemistry of the Faculty of Mathematics and Natural Sciences, Universitas Sumatera Utara in 2004 and a Master of Science in Physical Chemistry from the Department of Chemistry of the Faculty of Mathematics and Natural Sciences, Universitas Gadjah Mada in 2010. She was awarded a doctorate in Chemistry from Universitas Sumatera Utara in 2019. She is currently a lecturer in Physical

Chemistry at the Department of Chemistry, Universitas Negeri Medan. Her research areas are catalysis, renewable energy, energy production from biomass, and zeolite modification. She has published several scientific articles in international journals and holds some patents.



Rahayu earned her bachelor's degree from the Department of Chemistry, Faculty of Mathematics and Natural Sciences, Universitas Negeri Medan. She is currently pursuing a master's degree in Chemistry at the Department of Chemistry, Faculty of Mathematics and Natural Sciences, Universitas Andalas. She has been active as a research assistant since 2019 at Universitas Negeri Medan, focusing on catalysts and renewable energy. She has co-authored several scientific articles in international

journals.